Anorthite megacrysts from island arc basalts

MITSUYOSHI KIMATA*, NORIMASA NISHIDA†, MASAHIRO SHIMIZU*, SHIZUO SAITO‡,
TOMOAKI MATSUI* AND YOJI ARAKAWA*

* Institute of Geoscience,
† Chemical Analysis Centre,
‡ Institute of Materials Sciences,
The University of Tsukuba, Ibaraki 305, Japan.

Abstract

Anorthite megacrysts are common in basalts from the Japanese Island Arc, and signally rare in other global fields. These anorthites are 1 to 3 cm in size and often contain several corroded Mg-olivine inclusions. The megacrysts generally range from $An_{94}Ab_4Ot_2$ to $An_{89}Ab_6Ot_5$ (Ot: other minor end-members, including $CaFeSi_3O_8$, $CaMgSi_3O_8$, $AlAl_3SiO_8$, $\square Si_4O_8$) and show no chemical zoning. They often show parting. Red-clouded megacrysts contain microcrystals of native copper with a distribution reminiscent of the shape of a planetary nebula. Hydrocarbons are also present, both in the anorthite megacrysts and in the olivines included within them. Implications of lateral variations in the Fe/Mg ratio of the included olivines, in Sr-content and in Sr-isotope ratio of the anorthite megacrysts with respect to the Japanese island arc, relate to mixing of crustal components and subducted slab-sediments into the basaltic magmas.

KEYWORDS: anorthite, megacryst, island a.c, Japan, basalt.

Introduction

THOUGH very common in the north-east part of the Japanese island arc and Izu-Bonin arc, anorthite megacrysts have never been found in other districts in Japan (Ishikawa, 1951). They are also rare in the rest of the world (Donaldson, 1975; Sinton et al., 1993). Since the discovery in 1991 of native copper within anorthite megacrysts (Murakami et al., 1991), research on such microinclusions has transformed our understanding of the geochemical processes that influence the compositions of arc magmas. Recent studies by Kimata and co-workers (e.g. Kimata et al., 1992, 1993) on red-clouded anorthite and labradorite megacrysts, reportedly equivalent to sunstone, have concentrated on geochemical and crystallographic aspects of the inclusions.
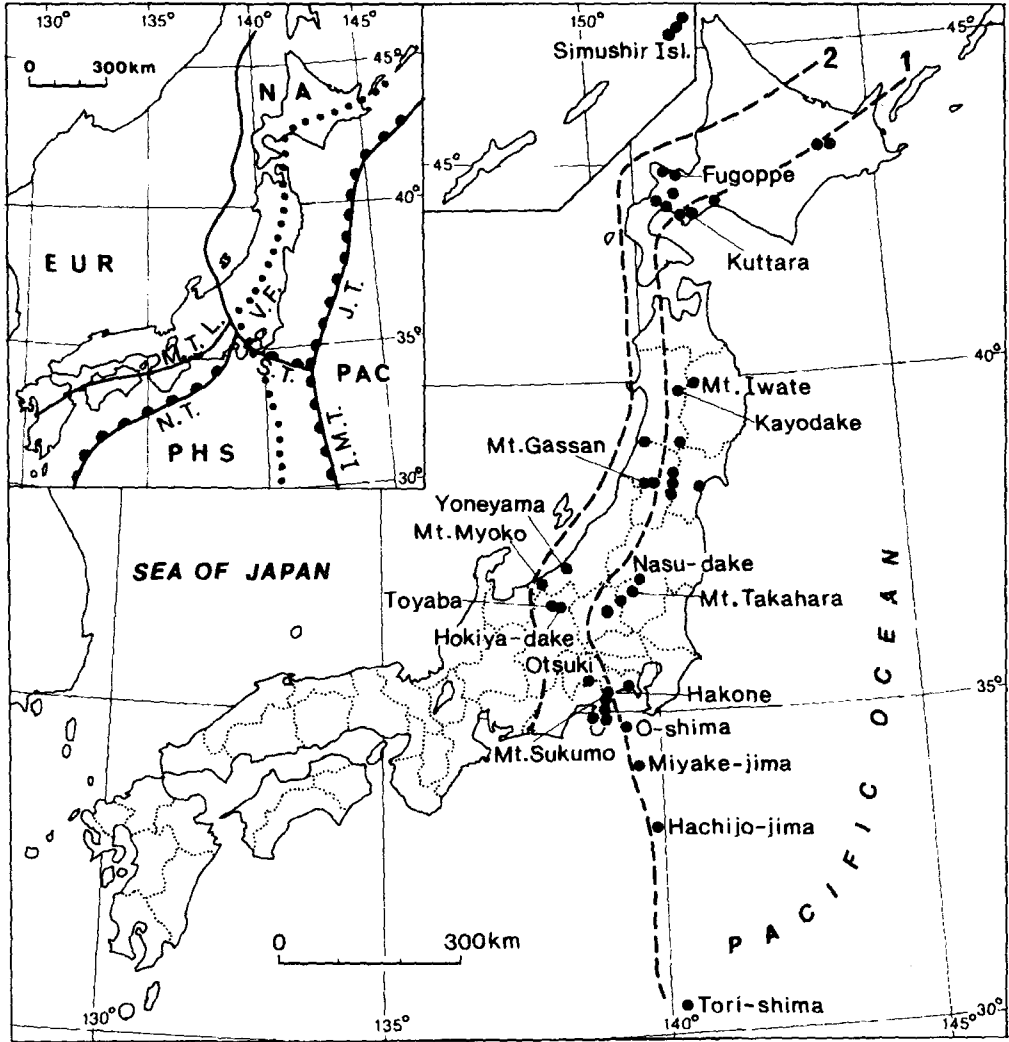
FIG. 1. Distribution of localities of anorthite megacrysts, modified after Ishikawa (1951). The left-upper map shows location of tectonic plates around Japanese Islands. Plates: EUR, Eurasia; NA, North America; PAC, Pacific; PHS, Phillipine Sea. Trench: J.T., Japan; I.M.T., Izu-Marianas. Trough: S.T, Sagami; N.T., Nankai; M.T.L., Median Tectonic Line; V.F., Volcanic Front. 1: boundary between tholeiite and high-Al basalt; 2: boundary between high-Al and alkaline olivine basalts.

This paper discusses the mineralogical and geochemical significance of anorthite megacrysts from basaltic rocks in the Japanese Island Arc, focusing on the migration of subduction components.

Sample localities

Occurrences of these anorthite megacrysts in Japan are shown in Fig. 1, and Kuno's definition (1966) enables us to group them into tholeiite and high-Al basalt zones. All the megacrysts are xenocrysts and occur in Neogene or Quaternary basaltic rocks (Ishikawa, 1951). Inclusions of native copper, zinc, chlorine and hydrocarbons have been discovered in the red-clouded anorthite megacrysts sampled from Hachijojima, one of the Seven Izu islands (Nishida et al., 1993; Kimata et al., 1993). Localities of anorthite megacrysts from Japanese and Izu-Mariana Island Arcs are on or along the volcanic front (upper-left in Fig. 1) identified by Sugimura (1960). The volcanic

front is built on the Philippine Sea and North American plates, which overlie the subducting Pacific plate.

Analytical methods

Each phase was examined under a petrographic microscope with high magnification, VANOX Olympus, and with powder or single crystal X-ray diffractometers (Rigaku automated powder type, RAD-C system, and an Enraf-Nonius CAD-4F type). High-temperature Fourier transform infrared microspectroscopy (FT-MIR) of Janssen-type and Raman scattering microspectroscopy (NR-1000) (both from Japan Spectroscopy) were used to identify microminerals (Kimata et al., 1991, 1993). Major and trace elements were determined for rock samples using X-ray fluorescence (Rigaku RIX2000). Chemical compositions of minerals were determined by electron microprobe analysis (JEOL JXA-8621) (Kimata et al., 1991), and by inductively coupled plasma-atomic emission spectrometry (ICP-AES; Jarrell-Ash Model 975 plasma atom comp). The chemical shift of characteristic X-ray lines for elements was estimated by EPMA in order to evaluate their coordination states (Murakami et al., 1991). $^{87}Sr/^{86}Sr$ isotopic compositions were measured on a Finnigan MAT 262 mass spectrometer equipped with five Faraday collectors (Arakawa et al., 1992).

Results and discussion

Morphology and colour. The principal habits of anorthite megacrysts are illustrated in Fig. 2. All the crystals are euhedral and usually more than 10 mm in diameter although exceptionally they can reach 40 mm. They are neither tabular (growth parallel to (010)), nor elongate in the direction of the c-axis. The morphology shown in Fig. 2a is typical of anorthite megacrysts from island arcs, and penetration twinning is commonly observed.

Anorthite megacrysts fall into three colour categories: (1) colourless, (2) red-clouded and (3) yellow. The present field survey confirms that red-clouded anorthites are from the volcanos of the Izu island arc, across the central part of Japan to Mt. Myoko (Hachijojima, Miyakejima, Ohshima, Hokiyadake, etc.), and yellow anorthites are from the same zone: Hakone and Hokiyadake volcanoes.

Microscopic observation. Definite partings are common to all the anorthite megacrysts examined (Fig. 3). A rare observation in thin section is that fluid microinclusions are arranged parallel to the faces of some anorthite crystals (Fig. 4) and form irregular patches. No optical zoning is evident in the megacrysts.

Most of the megacrysts contain corroded olivine (Fig. 5), and dislocation substructures are plainly visible within some of these (Fig. 6). An irregular network of dislocations with many bubbles (up to several um in diameter) has also been observed occasionally in olivine included within the megacrysts from Hachijojima.

X-ray crystallography. Cell parameters of the anorthite, as determined from X-ray diffraction data from single crystals, are summarised in Table 1. Very little variation is observed between the samples and the values are consistent with the crystals having a high degree of Al/Si order (Benna et al., 1985).

Chemical composition. No systematic difference in An or Ab contents has been found between megacrysts (Table 2). The samples of this suite also contain four minor end-member components: $CaFeSi_3O_8$, $CaMgSi_3O_8$, $Al(Al_3Si)O_8$ and $\square Si_4O_8$. Use of these six end-members for labradorites and synthetic Ca-rich plagioclases provides an adequate
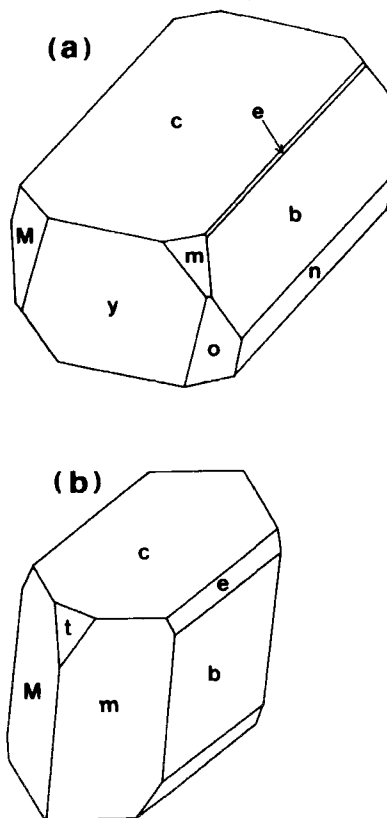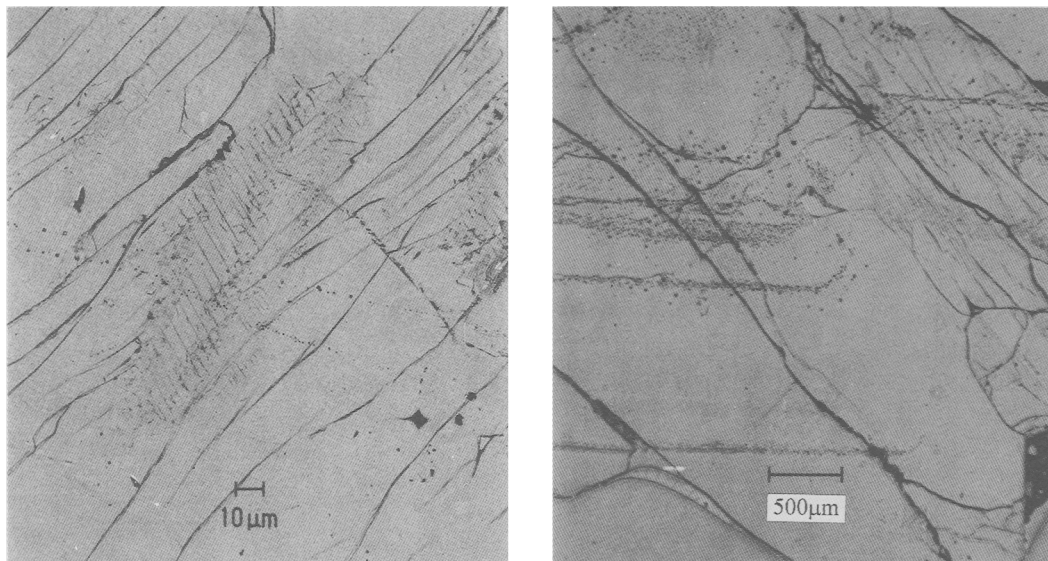

FIG. 2. Representative habits of anorthite megacrysts from (a) Kuttara and (b) Tonosawa (Hakone), Japanese islands. b(010), c(001), e(021), m(110), M(1$\bar{1}$0), n(02$\bar{1}$), o(111), t(201), y(20$\bar{1}$).

FIGS. 3 and 4. Fig. 3 (*left*) Transmitted-light photomicrograph of the red-clouded anorthite from Hachijojima, showing the characteristic partings. Fig. 4 (*right*) Photomicrograph showing the zones of fluid inclusions arranged parallel to the faces of anorthite crystal from Hachijojima.

description of their complete solid solution (Kimata et al., 1992; Murakami et al., 1992).

Representative microprobe analyses of corroded olivines included in the megacrysts reveal that their compositions range from $Fo_{83}Fa_{17}$ to $Fo_{75}Fa_{25}$ (Table 3). No chemical zoning was found across the single crystals. The MnO contents are less than 0.40 wt.%, whereas the CaO contents vary from 0.16–0.33 wt.%. Low Ca and Mn contents in olivines may indicate the effects of metastable crystallization and the bulk chemistry of the host magma (Brown, 1982).

Infrared spectroscopy. High-temperature infrared spectra for anorthite megacrysts from Miyakejima are shown in Fig. 7. Characteristic bands at 2930 and 2860 cm^{-1} assigned to CH_2-stretching vibrations (Colthup et al., 1975) have previously been observed in spectra of anorthite from Hachijojima (Kimata et al., 1993) and Ohshima. The sharp decrease in absorption intensity of major peaks above 240°C (Fig. 7) is due to lattice relaxation around the *M*-cation sites associated with the co-elastic $P\bar{1} \rightleftharpoons I\bar{1}$ transition (Salje, 1993). Recent studies using EPR spectroscopy has revealed the existence of feldspar with CH_4 radicals at K sites (Petrov et al., 1993). The structure of $[(CH_3)_3Si]_{14}[Si_7O_{21}]$, has been determined (Smolin et al., 1993) by comparison with $Ba_7[Si_7O_{21}]_{10}BaCl_2^-$ (Winkler et al., 1983). It is evident from this structural derivative that some hydrocarbons can substitute for alkali earth cations. In addition, the infrared absorption spectra for Miyakejima and Hachijojima anorthites are not consistent with spectra of the compound CH_3CuH (Billups et al., 1980).

The observation of hydrocarbons in corroded olivines is new (Fig. 8). The same hydrocarbons as in red-clouded anorthites exist as microinclusions in olivines or their constituents. A superficial difference in IR absorption intensity indicates that hydrocarbons are less abundant in olivines than in anorthites, differing by a factor of approximately ten in concentration. The present observation indicates that the magmas from which the anorthites and olivines crystallised contained the same hydrocarbons.

Native copper. Backscattered electron images of metallic microinclusions in a red-clouded anorthite megacryst from Hachijojima are given in Fig. 9. These inclusions identified as native copper applying the chemical shift method by EPMA. The small satellite inclusions seen in Fig. 9 are also native copper. The red-clouded state is due to optical scattering by micron sized grains of native copper. They have a distribution analogous to a planetary nebula (Fig. 9), and are quite different in morphology from the native copper commonly observed within other calcic plagioclases (Andersen, 1917; Hofmeister and Rossman, 1985; Murakami et al., 1991; Kimata et al., 1992; Nishida et al., 1994). The microscopic texture might be attributed to Ostwald ripening, with several copper 'satellites' becoming continuously incorporated into the larger crystal of a single disk-like film.
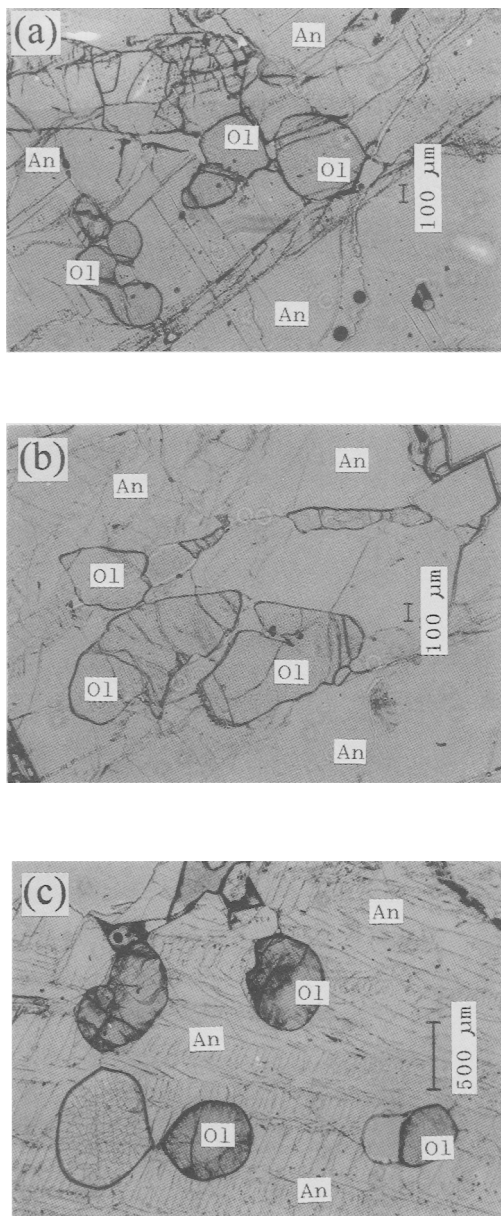
FIG. 5. Photomicrographs of the corroded olivines included by anorthite megacrysts from the Japanese Island Arc. (*a*) Kuttara, (*b*) Myoko and (*c*) Hchijojima. An, anorthite; Ol, olivine.

FIG. 6. Photomicrographs showing dislocations of the corroded olivine extracted from anorthite megacryst from Hachijojima.

Microinclusions in the corroded olivines. Microinclusions within the corroded olivines generally have subspherical/ellipsoidal shapes with boundaries modified to a subplanar 'negative crystal'-like outline (Fig.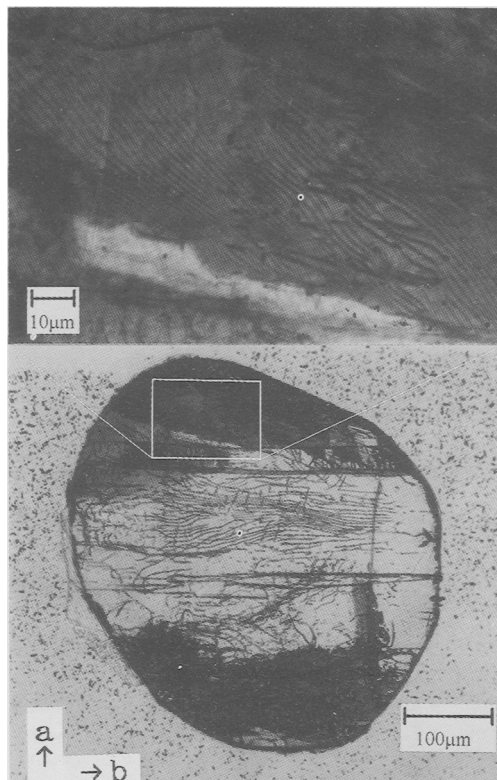 10). EPMA and Raman scattering microspectroscopy indicate that these microinclusions are Al-rich pyroxenes (fassaite and bronzite), together with aluminous spinels (Table 4). These minerals probably crystallized from a melt inclusion, which must have been the primary Al-rich magma.

Tectonic significance of characteristic anorthite megacryst chemistry. The Sr content of the anorthite megacrysts, determined by ICP analysis, increases with increasing distance from the Japan Trench (Fig. 11). As they become more distant from the trench, their $^{87}Sr/^{86}Sr$ ratios also tend to increase (Fig. 12). These two spatial trends are equivalent to the lateral variations observed in Quaternary volcanic rocks from the Northeast Japan Arc (Notsu, 1983). The Sr isotope ratios fall between the average values of MORB (0.7028) and of bulk earth (0.7047) (Vukadinovic, 1993). The data for anorthite megacrysts diverge from the view (Arculus and Johnson, 1981) that the Sr enrichment, or 'spike,' in arc volcanic rocks does not correlate positively with $^{87}Sr/^{86}Sr$. These differences in $^{87}Sr/^{86}Sr$ of anorthites, therefore, may imply contributions to the arc basalt

TABLE 1. Cell parameters of anorthite megacrysts from the Izu–Japan island arc system

Sample*	$a(\text{Å})$	$b(\text{Å})$	$c(\text{A})$	$\alpha(°)$	$\beta(°)$	$\gamma(8)$	$V(\text{Å}^3)$
HC	8.179(1)	12.877(2)	14.179(1)	93.20(2)	115.89(1)	91.19(1)	1339.7(1)
MY	8.179(1)	12.885(1)	14.177(1)	93.21(1)	115.89(1)	91.19(1)	1340.3(1)
OH	8.172(3)	12.878(4)	14.166(6)	93.22(2)	115.87(2)	91.18(2)	1337.7(9)
TN	8.179(2)	12.877(2)	14.177(4)	93.17(1)	115.90(1)	91.22(1)	1339.4(5)
SKG	8.181(1)	12.875(2)	14.173(3)	93.20(1)	115.88(1)	91.20(1)	1339.3(4)
SKY	8.180(1)	12.873(2)	14.176(3)	93.21(1)	115.91(1)	91.18(1)	1338.8(4)
OT	8.179(1)	12.875(2)	14.176(3)	93.20(1)	115.88(1)	91.19(1)	1339.2(4)
HK	8.181(1)	12.875(2)	14.177(3)	93.20(1)	115.91(1)	91.18(1)	1339.4(4)
TY	8.180(2)	12.875(2)	14.177(3)	93.22(1)	115.89(1)	91.18(1)	1339.6(4)
MK	8.181(2)	12.869(2)	14.172(3)	93.19(1)	115.92(1)	91.20(1)	1338.1(4)
YN	8.182(2)	12.879(2)	14.181(3)	93.19(1)	115.91(1)	91.18(1)	1340.3(4)
TK	8.172(2)	12.872(2)	14.166(4)	93.20(1)	115.88(1)	91.20(1)	1336.9(5)
NSN	8.170(2)	12.865(2)	14.177(3)	93.30(1)	115.90(1)	91.18(1)	1336.5(5)
GS**	8.169(1)	12.872(2)	14.222(2)	93.43(1)	116.23(1)	90.16(1)	1338.3(3)
IW	8.182(2)	12.874(2)	14.179(3)	93.25(1)	115.89(1)	91.14(1)	1339.8(4)
KY	8.179(2)	12.876(2)	14.174(4)	93.21(1)	115.89(1)	91.17(1)	1339.2(6)
FG	8.182(2)	12.875(2)	14.173(3)	93.20(1)	115.86(1)	91.21(1)	1339.5(5)
KT	8.180(2)	12.872(2)	14.174(3)	93.20(1)	115.90(1)	91.22(1)	1338.6(5)

* Abbreviation: HC, Hachijo-jima; MY, Miyake-jima; OH, O-shima; TN, Tonosawa (Hakone); SKG, Sukumogawa (Hakone); SKY, Sukumoyama (Izu); OT, Otsuki; HK, Hokiyadake; TY, Toyaba; MK, Mt. Myoko; YN, Yoneyama; TK, Mt. Takahara; NSN, Mt. Nangetsu (Nasu); GS, Mt. Gassan; IW, Mt. Iwate; KY, Kayodake; FG, Fugoppe; KT, Kuttara.

* * Plagioclase megacryst of $An_{47}Ab_{48}Or_2Ot_3$ composition.

magmas from either continental crust, [87]Sr-rich subducted material and/or enriched mantle lithosphere.

The Fe/Mg ratio of included olivines within the anorthite crystals increases with increasing distance from the Japan Trench to the back-arc side (Fig. 13), whereas the FeO/MgO ratio of Quaternary basalts in the Japanese Islands decreases from the volcanic front toward the back-arc side (Kushiro, 1983). The systematic contrast may be explained by crystallization of the included olivines from a primary magma which was different in chemistry from these Quaternary basalts.

Petrochemical background. Whole-rock analyses (Table 5) were performed on samples from which anorthite megacrysts had been removed. The rocks can be divided into tholeiites and high-Al basalts, and the grouping is consistent with the zones defined by Kuno (1966) (Fig. 1). A vanadium abundance of ~100–190 ppm is characteristic of the rocks, but is lower than found in MORB from the Mid-Atlantic Ridge (>250 ppm; Wilson, 1993). Vanadium, one of the compatible elements, is important in the identification of primary magma compositions. The present V concentration must reflect both the chemical composition of the mantle source and the partial melting processes involved in their formation.

Mineralogical background to anorthite crystallization. The processes by which anorthite megacrysts in the tholeiitic basalts are formed remain poorly constrained. Experimentally determined phase relations for the forsterite–anorthite system (Kushiro and Yoder, 1966), and melts of olivine tholeiite composition (Irving and Green, 1970) seem to require solidification of the parent basic magma at $P < 9$ kbar and T around 1200°C to give anorthite megacrysts and their included olivines. The lack of amphibole inclusions, however, implies that a depth of greater than 20 km is necessary for the genesis of these megacrysts (Pawley and Holloway, 1993). The orientation of the fluid inclusions relative to the growth direction of the host crystal (Fig. 4) points to the importance of fluids for megacrystallization of the anorthites. Sisson and Grove (1993) addressed the formation of very calcic plagioclase (>An_{90}) from basaltic melts with high H_2O contents. The deformation features in the corroded olivines (Fig. 6) bear a close resemblance to those of dislocations generated by high strain rates over a wide temperature range up to 1200°C (Buiskool Toxopeus and Boland, 1976). Fluids would enhance the rate of dislocation climb (Mackwell, 1985). Plagioclase accumulation is a pervasive process in arc magmas (Crawford et al., 1987). Sea water and slab-sediments

TABLE 2. Representative microprobe analyses of anorthite megacrysts from the Izu–Japan island arc system

Sample*	HC	MY	OH	TN	SKG	SKY	OT	HK	TY	MK	YN	TK	NSN	IW	KY	FG	KT
SiO_2	44.04	44.49	44.91	44.13	44.23	44.82	43.95	45.43	44.75	44.96	44.29	44.12	44.74	45.06	44.95	44.34	44.47
Al_2O_3	35.23	35.15	34.94	35.54	35.45	35.24	35.42	35.35	35.01	35.32	35.78	35.08	35.31	34.32	34.83	35.38	35.49
FeO**	0.43	0.37	0.63	0.40	0.37	0.52	0.36	0.50	0.48	0.46.	0.56	0.41	0.51	0.41	0.55	0.44	0.49
MgO	0.10	0.12	0.12	0.05	0.06	0.09	0.08	0.10	0.07	0.05	–	–	0.09	–	0.08	0.10	–
CaO	19.12	18.84	18.69	19.37	19.25	19.03	19.32	18.59	18.89	19.13	19.06	19.12	18.77	18.30	18.70	19.17	18.83
Na_2O	0.40	0.49	0.44	0.36	0.44	0.58	0.34	0.65	0.54	0.57	0.39	0.47	0.53	0.87	0.71	0.41	0.42
Total	99.32	99.46	99.73	99.89	99.80	100.28	99.47	100.62	99.74	100.49	100.08	99.20	99.95	98.96	99.82	99.75	99.71

Numbers of ions on the basis of 8 O

	HC	MY	OH	TN	SKG	SKY	OT	HK	TY	MK	YN	TK	NSN	IW	KY	FG	KT
Si	2.051	2.066	2.079	2.045	2.050	2.066	2.044	2.083	2.073	2.069	2.045	2.054	2.067	2.099	2.081	2.054	2.058
Al	1.934	1.924	1.907	1.935	1.937	1.915	1.941	1.910	1.911	1.915	1.948	1.925	1.923	1.885	1.900	1.931	1.937
Fe**	0.017	0.015	0.024	0.015	0.015	0.020	0.014	0.019	0.019	0.018	0.022	0.016	0.020	0.016	0.021	0.017	0.019
Mg	0.007	0.008	0.008	0.004	0.004	0.006	0.006	0.007	0.005	0.003	–	–	0.006	–	0.006	0.007	–
Ca	0.954	0.958	0.927	0.962	0.956	0.940	0.963	0.913	0.937	0.943	0.943	0.954	0.929	0.914	0.927	0.951	0.934
Na	0.036	0.044	0.040	0.036	0.040	0.052	0.031	0.058	0.049	0.051	0.035	0.042	0.048	0.079	0.064	0.037	0.038
Total	4.999	4.994	4.985	5.003	5.002	4.999	4.999	4.990	4.994	4.999	4.993	4.993	4.993	4.993	4.999	4.999	4.986
An***	93.0	93.8	89.5	94.3	93.6	91.4	93.0	88.7	91.3	92.2	92.1	93.8	90.3	89.9	90.0	92.7	91.5
Ab	3.6	4.0	4.0	3.6	4.0	5.2	3.6	5.8	4.9	5.1	3.5	4.2	4.8	7.9	6.4	3.7	3.8
CF	1.7	1.5	2.4	1.6	1.5	2.0	1.7	1.9	1.9	1.8	2.2	1.6	2.0	1.6	2.1	1.7	1.9
CM	0.7	0.5	0.8	0.3	0.4	0.6	0.7	0.7	0.5	0.3	–	–	0.6	0.4	0.6	0.7	–
CS	–	0.2	1.4	–	–	–	–	0.9	0.5	0.1	0.4	0.1	0.6	0.4	–	0.2	1.0
AS	1.0	–	1.9	0.5	0.6	0.9	1.0	2.0	0.9	0.5	1.8	0.2	1.7	0.3	0.9	1.0	1.7
Total	100.0	100.0	100.0	100.3	100.1	100.1	100.0	100.0	100.0	100.0	100.0	99.9	100.0	100.1	100.0	100.0	99.9

* Abbreviation of sample names is as in Table 1.

** Total iron as FeO.

*** Contraction of end-members: An $CaAl_2Si_2O_8$; Ab, $NaAlSi_3O_8$; CF, $CaFeSi_3O_8$; CM, $CaMgSi_3O_8$; CS, $\square Si_4O_8$; AS, $Al(Al_3Si)O_8$
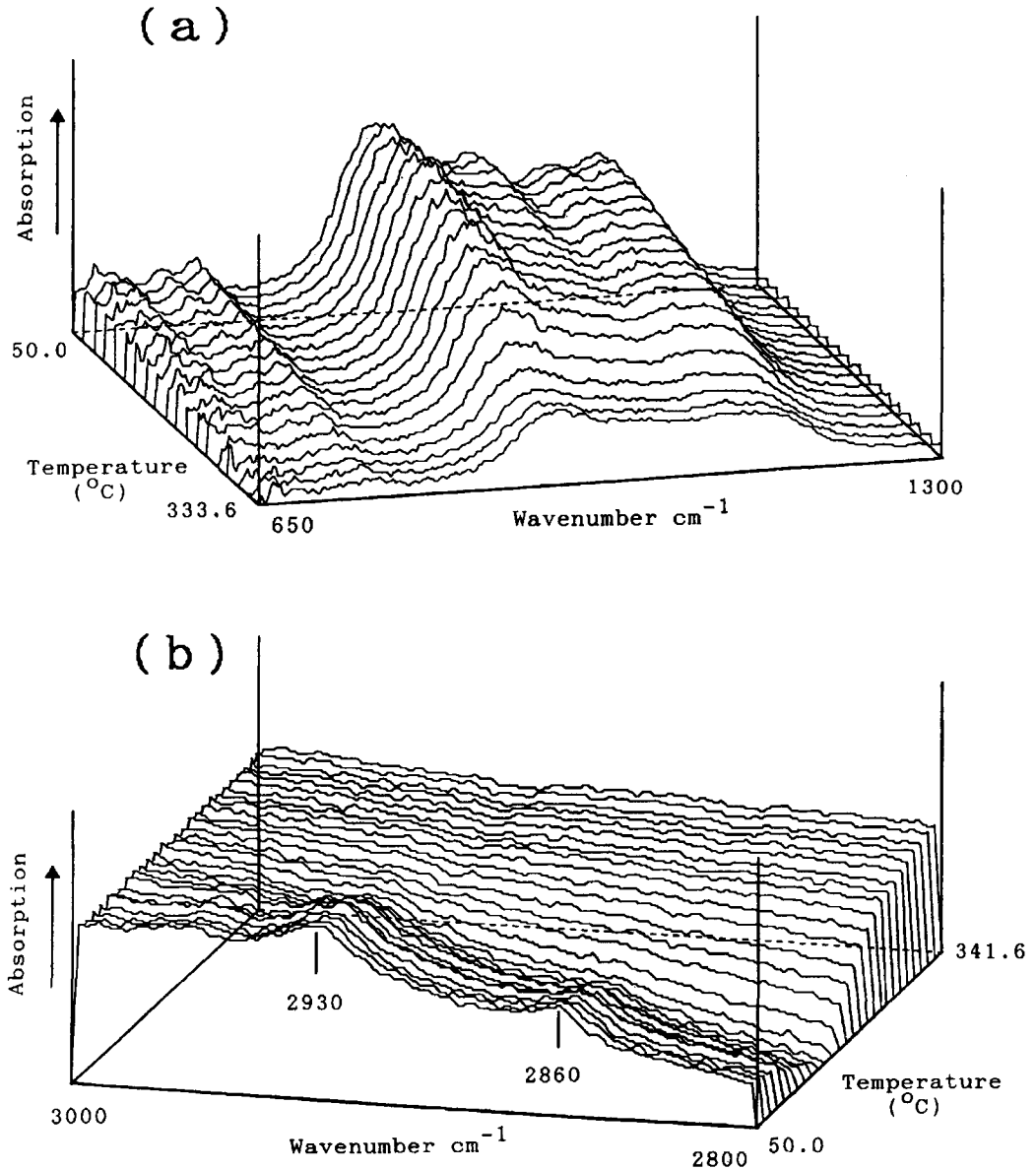
FIG. 7. Infrared microspectra for Miyakejima anorthite in the regions (*a*) 1300–650 and (*b*) 3000–2800 cm^{-1} between 50°C and 340°C.

rich in clay minerals, which would appear to be the source of metals and excess Al- and Si-components for anorthite megacryst formation, would be entrained easily into the magma chamber by an escalator transport type of mechanism (Davies and Stevenson, 1992). The viewpoint that CH$_4$ and Cl activate the generation of partial melts in the upper mantle (Foley *et al.*, 1986) is supported by the present paragenesis of hydrocarbons and chlorine within anorthite megacrysts.

The growth of anorthite is favoured by the addition of Al$_2$O$_3$ to basaltic magma (Bowen, 1922). Physical

TABLE 3. Representative microprobe analyses of the corroded olivines included in anorthite megacrysts

Sample*	HC	MY	OH	SKY	TY	MK	TK	NSN	KT
SiO_2	39.38	39.11	39.54	39.14	38.10	38.60	39.12	39.61	38.74
Al_2O_3	–	–	0.24	–	–	–	–	–	–
FeO	16.79	15.81	16.32	17.02	22.28	20.48	16.99	16.95	21.13
MnO	0.37	0.27	0.30	0.23	0.37	0.31	0.25	0.29	0.30
NiO	0.09	–	–	–	–	–	–	–	–
MgO	42.77	44.17	43.06	42.68	38.43	40.20	42.57	43.08	39.31
CaO	0.23	0.19	0.33	0.22	0.16	0.16	0.16	0.18	0.20
Total	99.63	99.55	99.79	99.29	99.34	99.75	99.09	100.11	99.85

Numbers of ions on the basis of 4 (O)

| Si	1.002	0.991	1.001	0.999	0.998	0.997	0.993	1.002	1.002
Al	–	–	0.007	–	–	–	–	–	–
Fe	0.357	0.335	0.345	0.363	0.488	0.442	0.354	0.358	0.457
Mn	0.008	0.006	0.007	0.005	0.008	0.007	0.005	0.006	0.007
Ni	0.002	–	–	–	–	–	–	–	–
Mg	1.622	1.668	1.625	1.624	1.500	1.547	1.646	1.624	1.516
Ca	0.006	0.005	0.009	0.006	0.004	0.005	0.005	0.005	0.006
Total	2.997	3.005	2.994	2.997	2.998	2.998	3.003	2.995	2.993
mg**	81.6	83.0	82.2	81.5	75.2	77.5	82.1	81.7	76.6

*   Abbreviation of samples is as in Table 1.
** mg $Mg/(Mg + Fe^{2+} + Mn)$.
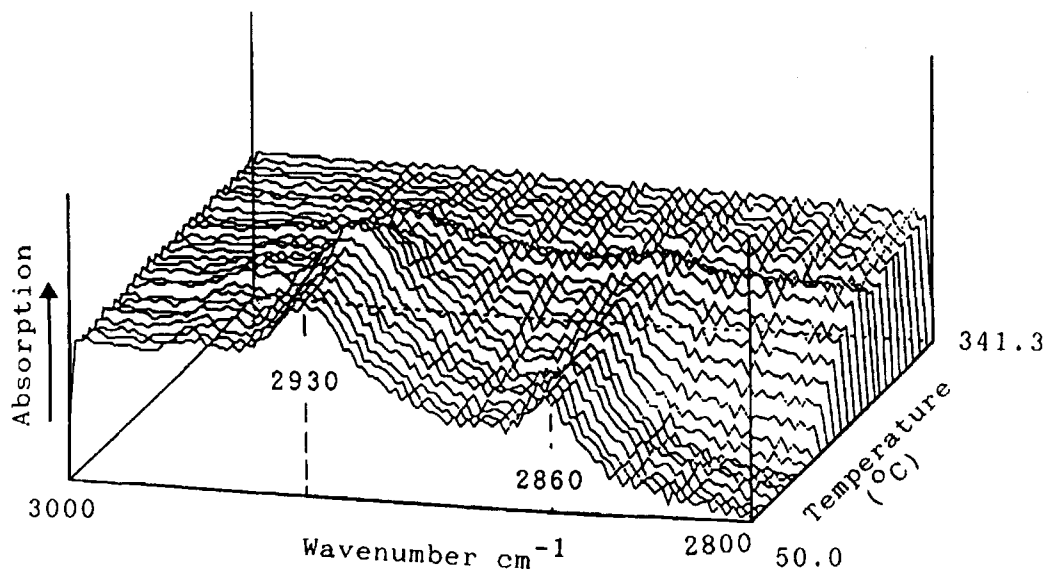
FIG. 8. Infrared microspectra of the corroded olivines included in anorthite megacrysts from Hachijojima in the region 3000–2800 cm^{-1} between 50°C and 340°C.

M. KIMATA *ET AL.*

TABLE 4. Representative microprobe analyses of aluminous Mg-pyroxenes (PX) and spinel (Sp) included by the corroded olivine in an anorthite megacryst (Fig. 10)

Sample	PX-1	PX-2	PX-3	PX-4	Fassaite	Bronzite	Sp
SiO_2	45.51	42.89	46.88	47.72	46.00	47.30	–
TiO_2	0.64	1.05	0.32	0.31	0.25	0.63	0.55
Al_2O_3	10.72	13.25	11.52	11.10	9.50	10.81	9.86
Fe_2O_3	–	–	–	–	5.69	7.80	64.22
FeO	9.49	10.48	13.52	12.90	1.51	9.20	20.12
MnO	0.28	0.23	0.26	0.30	0.08	0.03	0.35
MgO	12.16	10.58	24.66	26.02	12.37	23.60	5.94
CaO	20.20	20.57	1.54	1.63	24.75	0.28	–
Na_2O	0.19	0.22	–	–	0.05	–	–
Total	99.19	99.27	98.70	99.98	100.20	99.71	101.04

Numbers of ions on the basis of 6 (O) or 4(O)

Si	1.716	1.631	1.709	1.713	1.704	1.703	–
Ti	0.018	0.030	0.009	0.008	0.007	0.017	0.014
Al	0.477	0.594	0.493	0.470	0.415	0.459	0.403
Fe^{3+}	–	–	–	–	0.159	0.211	1.538
Fe^{2+}	0.299	0.333	0.412	0.387	0.047	0.277	0.725
Mn	0.009	0.008	0.008	0.009	0.003	0.001	0.011
Mg	0.684	0.599	1.340	1.392	0.683	1.266	0.308
Ca	0.816	0.838	0.060	0.063	0.983	0.011	–
Na	0.014	0.016	–	–	0.004	–	–
Total	4.033	4.049	4.031	4.042	4.005	3.945	2.999

* Fassaite: fassaite-diopside metasomatized dolerite, Vilyuy (Ginzburg, 1969).
** Bronzite: pyrope-sapphirine rock (Lutts & Kopaneva, 1968).
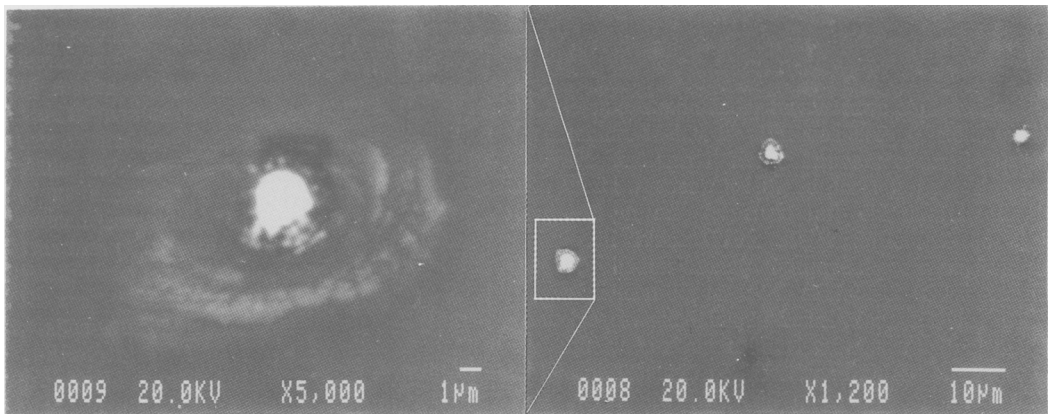

FIG. 9. Composite backscattered electron micrographs of a polished thin section of native coppers (white) included in an anorthite megacryst from Hachijojima.
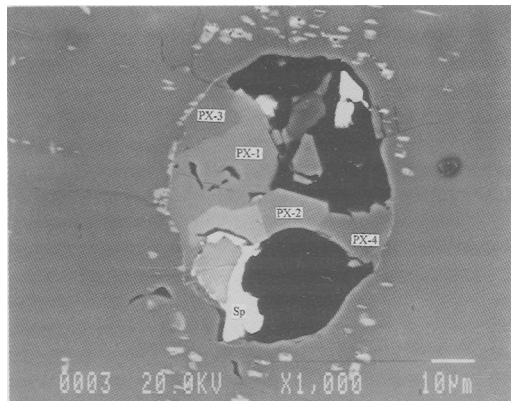
FIG. 10. Backscattered electron micrograph of Al-rich pyroxenes and spinels in the corroded olivine included by anorthite megacryst. PX-1 etc. are as in Table 4.

conditions produced by contamination might perhaps aid the growth of large crystals, in the same way that clay mixed in salt water leads to the better growth of salt crystals (Koide and Nakamura, 1943). Evidence for these effects may be provided by the following observations: viscosity not only increases with the mole fraction of SiO_2 (e.g. compilations in Bottinga and Weil, 1972) but also with that of Al_2O_3

(Riebling, 1966). The rapid growth of anorthite megacrysts requires both the addition of Al_2O_3 and dissolution of excess SiO_2 into the basaltic melt. Thermochemistry of glasses and liquids in the $CaAl_2O_4$–SiO_2 system (Navrotsky et al., 1982) is consistent with this. Heats of solution (ΔH_{sol}) and of mixing (ΔH_{mix}) in the system reach a pronounced minimum at $Al/(Al+Si)$ slightly greater than 0.5, resulting from enhanced stability of Si–O–Al bridging bonds relative to Si–O–Si and Al–O–Al. Furthermore the four-membered tetrahedral rings in the crystal structure of anorthite $Ca[Al_2Si_2O_8]$ are believed to exist also in the equivalent glass (Taylor and Brown, 1979). Reviews of the growth rates of plagioclases (Smith and Brown, 1988) reveal that the maximum growth rate for anorthite is much larger than that of albite. Artificial melts of $Ab_{70}An_{30}$ held at 1200°C with a CuO catalyser yielded the bladed aggregates with C-twins more than several mm long (Gorai, 1965). Each effect, of sea water, copper, subducted sediments rich in clay minerals and hydrocarbons, promotes a geochemical balance between the crystallization of anorthite megacrysts and the generation of partial melts.

In combination, the present results suggest that the formation of anorthite megacrysts may be linked to subducted sediments rich in H_2O, CO_2, Cl, hydrocarbons and metals accelerating the genesis of arc magmas.

TABLE 5. Major and trace element contents of the tholeiite series lavas characterized by the presence of anorthite megacrysts

Sample*	HC	MY	SKG	MK	TK	KY	KT
SiO_2	47.07	51.14	51.69	51.82	49.78	50.09	52.50
TiO_2	0.52	1.03	0.79	0.90	0.67	0.90	0.61
Al_2O_3	17.16	16.61	18.70	19.25	21.15	20.11	18.00
Fe_2O_3	11.87	12.54	10.64	9.93	9.56	11.15	11.21
MnO	0.18	0.19	0.17	0.16	0.14	0.17	0.17
MgO	11.13	6.13	5.25	4.89	5.54	4.60	6.00
CaO	11.17	10.13	10.69	9.84	11.66	11.09	9.65
Na_2O	1.24	2.25	2.03	2.47	1.70	2.35	1.98
K_2O	0.09	0.43	0.36	1.23	0.21	0.25	0.25
P_2O_5	0.04	0.12	0.08	0.24	0.09	0.10	0.06
Total	100.47	100.57	100.40	100.73	100.50	100.81	100.43
ppm							
Cr	98.0	40.7	67.6	38.7	145.2	67.7	61.6
Ba	25.4	209.4	197.1	232.4	95.4	124.1	118.4
Sr	166.0	251.3	257.0	415.4	305.5	344.3	263.3
V	108.1	187.7	152.9	159.3	126.5	165.9	118.7
KC**	TH	TH	TH	HA	TH	TH	TH

* Abbreviation of names for rock samples is as in Table 1.
** Kuno's classification (1966): TH, tholeiite; HA, high-Al basalt.
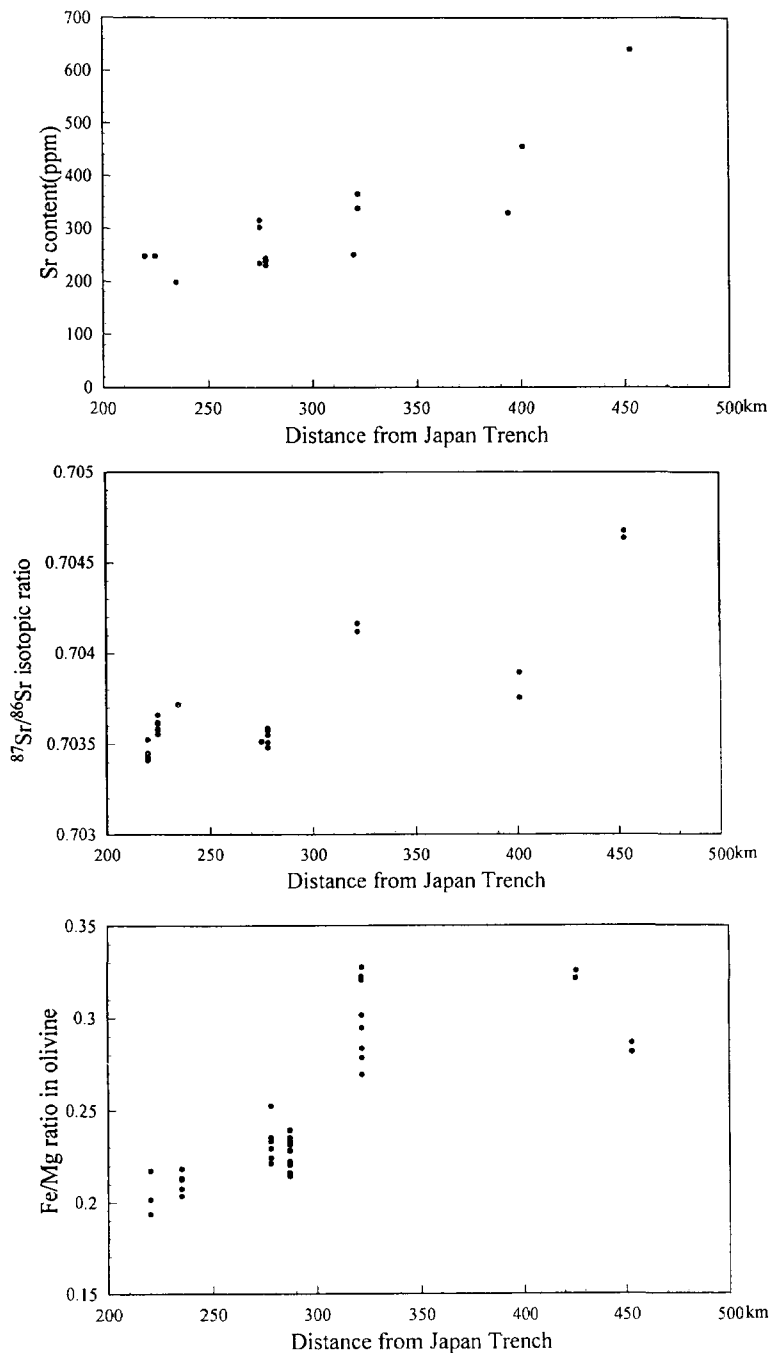
FIGS. 11–13. Fig. 11 (*top*) Variation of SrO content (ppm) of anorthite megacrysts versus their distances from the Japan Trench. Fig. 12 (*middle*) $^{87}Sr/^{86}Sr$ isotopic data for anorthite megacrysts plotted against their distances from the Japan Trench. Fig. 13 (*bottom*) Variation of Fe/Mg in the included olivine with their distances from the Japan Trench.

Acknowledgements

References

Andersen, O. (1917) Aventurine feldspar from California. *Amer. Mineral.*, **2**, 91.

Arakawa Y., Murakami, H., Kimata, M. and Shimoda, S. (1992) Strontium isotope compositions of anorthite and olivine phenocrysts in basaltic lavas and scorias of Miyakejima volcano, Japan. *J. Min. Pet. Econ. Geol.*, **87**, 226–39.

Arculus, R. J. and Johnson, R. W. (1981) Island arc magma sources: A geochemical assessment of the roles of slab-derived components and crustal contamination. *Geochem. J.*, **15**, 109–33.

Benna, P. Zanini, G. and Bruno, E. (1985) Cell parameters of thermally treated anorthite. Al,Si configurations in the average structures of the high temperature calcic plagioclases. *Contrib. Mineral. Petrol.*, **90**, 381–5.

Billups, W. E., Konarski, M. M., Hauge, R. H. and Margrave, J. L. (1980) Activation of methane with photoexcited metal atoms. *J. Amer. Chem. Soc.*, **102**, 7393–4.

Bottinga, Y. and Weil, D. F. (1972) The viscosity of magmatic silicate liquids: a model for calculation. *Amer. J. Sci.*, **272**, 438–75.

Bowen, N. L. (1922) The behavior of inclusions in igneous rocks. *J. Geol.*, **30**, 513–70.

Brown, G. E. Jr. (1982) Olivines and silicate spinels. In Miner. Soc. Amer., *Reviews in Mineralogy*, **5**, 275–392.

Buiskool Toxopeus, J. M. A. and Boland, J. N. (1976) Several types of natural deformation in olivine, an electron microscope study. *Tectonophys.*, **32**, 209–33.

Colthup, N. B., Daly, L. H. and Wiberly, S. E. (1975) *Introduction to Infrared and Raman Spectroscopy*, 2nd edn. Academic Press.

Crawford, A. J., Falloon, T. J., and Eggins, S. (1987) The origin of island arc high-alumina basalts. *Contrib. Mineral. Petrol.*, **97**, 417–30.

Davies, J. H. and Stevenson, D. J. (1992) Physical model of source region of subduction zone volcanics. *J. Geophys. Res.*, **97**, 2037–70.

Donaldson, C. H. (1975) Ultramafic inclusions in anorthite megacrysts from the Isle of Skye. *Earth Planet. Sci. Lett.*, **27**, 251–6.

Foley, F. S., Taylor, W. R. and Green, D. H. (1986) The role of fluorine and oxygen fugacity in the genesis of the ultrapotassic rocks. *Contrib. Mineral. Petrol.*, **94**, 183–92.

Ginzburg, I. V. (1969) Immiscibility of the natural pyroxenes diopside and fassaite and the criterion for it. *Dokl. Acad. Sci. U.S.S.R., Earth Sci. Sect.*, **186**, 106–109.

Gorai, M. (1965) Twinning in some artificial plagioclases. *Indian Mineral.*, **6**, 51–4.

Hofmeister, A. M. and Rossman, G. R. (1985) Exsolution of metallic copper from Lake County labradorite. *Geology*, **13**, 644–47.

Irving, A. J. and Green, D. H. (1970) Experimental duplication of mineral assemblages in basic inclusions of the Delegate breccia pipes. *Phys. Earth Planet. Interior.*, **3**, 385–9.

Ishikawa, T. (1951) Petrological significance of large anorthite crystals included in some pyroxene andesites and basalts in Japan. *J. Fac. Sci., Hokkaido Univ.*, Ser. IV, Vol. VII, No.4, 339–54.

Kimata, M., Shimizu, M., Saito, S., Murakami, H. and Shimoda, S. (1991) Analytical process for microprobing the crystals in a thin section: Focused on Raman and Infrared absorption spectroscopies. *Ann. Rep. Inst. Geosci., Univ. Tsukuba*, no. 17, 85–92.

Kimata, M., Nishida, N., Shimizu, M., Saito, S. and Arakawa, Y. (1992) Geochemical roles of aventurine labradorites including native coppers: Implication for continental-margin magmatism. submitted to Pegmatite symposium of 'Lepidorite 200'.

Kimata, M., Shimizu, M., Saito, S., Nishida, N., Arakawa, Y. and Shimoda, S. (1993) Hydrocarbons within anorthite megacrysts as a window to understanding the arc-magmatic process. *Neues Jahrb. Mineral., Mh.*, 408–16.

Koide, H. and Nakamura, T. (1943): On the growth of crystals in the presence of colloids. *Proc. Imp. Acad. Tokyo*, **19**, 202–4.

Kuno, H. (1966) Lateral variation of basalt magma type across continental margins and island arcs. *Bull. Volcanol.*, **29**, 195–222.

Kushiro, I. (1983) On the lateral variations in chemical composition and volume of Quaternary volcanic rocks across Japanese arcs. *J. Volcanol. Geotherm. Res.*, **18**, 435–47.

Kushiro, I. and Yoder, H. S. (1966) Anorthite–forsterite and anorthite–enstatite reactions and their bearing on the basalt–eclogite transformation. *J. Petrol.*, **7**, 337–62.

Lutts, B. G. and Kopaneva, L. H. (1968) A pyrope-sapphirine rock from the Anabar massif and its conditions of metamorphism. *Dokl. Acad. Sci., U.S.S.R., Earth Sci. Sect.*, **179**, 161–3.

Mackwell, S. J. (1985) The role of water in the deformation of olivine single crystals. *J. Geophys. Res.*, 90, **B13**, 11319–33.

Murakami, H., Kimata, M. and Shimoda, S. (1991) Native copper included by anorthite, from the island of Miyakejima: implication for arc magmatism. *J. Min. Pet. Econ. Geol.*, 86, 364–74.

Murakami, H., Kimata, M., Shimoda, S., Ito, E. and Sasaki, S. (1992) Solubility of $CaMgSi_3O_8$ and $\square Si_4O_8$ endmembers in anorthite. *J. Min. Pet. Econ. Geol.*, **87**, 491–509.

Navrotsky, A., Peradeau, McMillan, P. and Coutoures, J. P. (1982): A thermochemical study of glasses and crystals along the joins silica–calcium aluminate and silica–sodium aluminate. *Geochim. Cosmochim. Acta*, **44**, 2039–49.

Nishida, N., Kimata, M. and Arakawa, Y. (1994) Native zinc, copper and brass in the red-clouded anorthite megacryst as probes of the arc-magmatic process. *Naturwissenschaften* (in press).

Notsu, K. (1983) Strontium isotope composition in volcanic rocks from the Northeast Japan arc. *J. Volcanol. Geothermal. Res.*, **18**, 531–48.

Pawley, A. R. and Holloway, J. R. (1993) Water Sources for subduction zone volcanism: new experimental constraints. *Science*, **260**, 664–6.

Petrov, I., Mineeva, R. M., Bershov, L. V. and Agel, A. (1993) EPR of $[Pb-Pb]^{3+}$ mixed valence pairs in amazonite-type microcline. *Amer. Mineral.*, **78**, 500–10.

Riebling, E. F. (1966) Structure of sodium aluminosilicate melts containing at least 50 mol% SiO_2 at 1500°C. *J. Chem. Phys.*, **44**, 2857–65.

Salje, E. K. H. (1993) *Phase transitions in ferroelastic and co-elastic crystals*, Student edn. Cambridge University Press, 229 pp.

Sinton, C. W., Christie, D. M., Coombs, V. L., Nielsen, R. L. and Fisk, M. R. (1993) Near-primary melt inclusions in anorthite phenocrysts from the Galapagos Platform. *Earth Planet. Sci. Lett.*, **119**, 527–37.

Sisson, T. W. and Grove, T. L. (1993) Temperatures and H_2O of low-MgO high-alumina basalts. *Contrib. Mineral. Petrol.*, **113**, 167–84.

Smith, J. V. and Brown, W. L. (1988) *Feldspar Minerals, 1. Crystal structures, Physical, Chemical, and Microtextural Properties*. Springer-Verlag, Berlin, 828 pp.

Smolin, Yu. I., Shepelev, Yu. F. and Ershov, A. S. (1993) The crystal structure of the trimethylsilyl derivative of the seven-membered ring silicate anion — $[(CH_3)_3Si]_{14}[Si_7O_{21}]$, *Z. Kristallogr.*, **203**, 73–8.

Sugimura, A. (1960) Zonal arrangement of some geophysical and petrological features in Japan and its environs. *J. Fac. Sci. Univ. Tokyo*, Sec. II, **12**, 133–53.

Taylor, M. and Brown, G. E. (1979) Structure of mineral glasses. I. The feldspar glasses $NaAlSi_3O_8$, $KAlSi_3O_8$, $CaAl_2Si_2O_8$. *Geochim. Cosmochim. Acta*, **43**, 61–77.

Vukadinovic, D. (1993) Are Sr enrichments in arc basalts due to plagioclase accumulation?. *Geology*, **21**, 611–4.

Wilson, M. (1993) *Igneous Petrogenesis*. Chapman & Hall, London, 466 pp.

Winkler, A., Hoebbel, D., Grimmer, A. R. and Wieker, W. (1983) $Ba_7[Si_7O_{21}]_{10}BaCl_2^-$ a compound with a new type of cyclic silicate anions. *Rev. Chim. Miner.*, **20**, 801–6.